AD-A186 353 TWO-DIMENSIONAL IMAGING MEASUREMENTS IN SUPERSONIC FLOWS USING LASER-INDU..(U) STANFORD UNIV CA HIGH TEMPERATURE GASDYNAMICS LAB L M COHEN ET AL. 10 JUN 87 1/1

UNCLASSIFIED AFOSR-TR-87-0986 $AFOSR-87-0057 F/G 9/3 NL

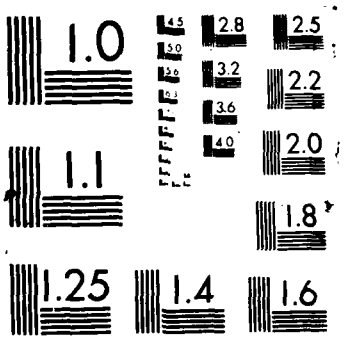
1.0
1.1
1.25
1.4
1.6
1.8
2.0
2.2
2.5
2.8
3.2
3.6
4.0
4.5
5.0

SECURITY CLASSIFICATION OF THIS PAGE - Unclassified

REPORT DOCUMENTATION PAGE

DTIC FILE COPY

AD-A186 353

1b. RESTRICTIVE MARKINGS

3. DISTRIBUTION/AVAILABILITY OF REPORT
Approved for public release; distribution is unlimited.

4. PERFORMING ORGANIZATION REPORT NUMBER(S)

5. MONITORING ORGANIZATION REPORT NUMBER(S)
AFOSR-TR- 87-0986

6a. NAME OF PERFORMING ORGANIZATION
Stanford University

6b. OFFICE SYMBOL (If applicable)

7a. NAME OF MONITORING ORGANIZATION
AFOSR/NA

6c. ADDRESS (City, State, and ZIP Code)
Department of Mechanical Engineering
Stanford, CA 94305

7b. ADDRESS (City, State, and ZIP Code)
Building 410, Bolling AFB DC
20332-6448

8a. NAME OF FUNDING/SPONSORING ORGANIZATION
AFOSR/NA

8b. OFFICE SYMBOL (If applicable)
NA

9 PROCUREMENT INSTRUMENT IDENTIFICATION NUMBER
AFOSR 87-0057

8c. ADDRESS (City, State, and ZIP Code)
Building 410, Bolling AFB DC
20332-6448

10 SOURCE OF FUNDING NUMBERS

PROGRAM ELEMENT NO.	PROJECT NO.	TASK NO.	WORK UNIT ACCESSION NO.
61102F	2308	A3	

11 TITLE (Include Security Classification)
Two-Dimensional Imaging Measurements in Supersonic Flows Using Laser-Induced Fluorescence of Oxygen

12 PERSONAL AUTHOR(S)
L. M. Cohen, M. P. Lee, P. H. Paul and R. K. Hanson

13a TYPE OF REPORT	13b. TIME COVERED	14. DATE OF REPORT (Year, Month, Day)	15. PAGE COUNT
Journal Reprint	FROM _____ TO _____	June 8-10, 1987	6

16 SUPPLEMENTARY NOTATION

17 COSATI CODES		
FIELD	GROUP	SUB-GROUP

18. SUBJECT TERMS (Continue on reverse if necessary and identify by block number)
Laser, Fluorescence, Imaging
Oxygen, Supersonic Flow, Excimer

19 ABSTRACT (Continue on reverse if necessary and identify by block number)

Planar laser induced fluorescence of molecular oxygen in a supersonic jet of heated air is reported. A tunable, narrow-bandwidth ArF excimer laser was used to excite a rovibronic transition of oxygen in the Schumann-Runge band system at 193 nm. A comparison between the predicted pressure and temperature profiles obtained in the underexpanded round jet with the fluorescence image data is presented.

DTIC
ELECTE
OCT 0 1 1987
D

20. DISTRIBUTION/AVAILABILITY OF ABSTRACT
☒ UNCLASSIFIED/UNLIMITED ☒ SAME AS RPT ☐ DTIC USERS

21 ABSTRACT SECURITY CLASSIFICATION
Unclassified

22a NAME OF RESPONSIBLE INDIVIDUAL
Julian M. Tishkoff

22b. TELEPHONE (Include Area Code)
(202)767-4935

22c OFFICE SYMBOL
AFOSR/NA

DD FORM 1473, 84 MAR 83 APR edition may be used until exhausted. All other editions are obsolete.

SECURITY CLASSIFICATION OF THIS PAGE
Unclassified

AIAA-87-1527
TWO-DIMENSIONAL IMAGING MEASUREMENTS IN SUPERSONIC FLOWS USING LASER-INDUCED FLUORESCENCE OF OXYGEN

L. M. Cohen, M. P. Lee,
P. H. Paul and R. K. Hanson,
Stanford University,
Stanford, CA 94305-3032

AIAA 22nd Thermophysics Conference
June 8-10, 1987/Honolulu, Hawaii

TWO-DIMENSIONAL IMAGING MEASUREMENTS IN SUPERSONIC FLOWS USING LASER-INDUCED FLUORESCENCE OF OXYGEN

L. M. Cohen, M. P. Lee, P. H. Paul and R. K. Hanson
High Temperature Gasdynamics Laboratory
Department of Mechanical Engineering
Stanford University
Stanford, CA 94305-3032

ABSTRACT

Planar laser induced fluorescence of molecular oxygen in a supersonic jet of heated air is reported. A tunable, narrow-bandwidth ArF excimer laser was used to excite a rovibronic transition of oxygen in the Schumann-Runge band system at 193 nm. A comparison between the predicted pressure and temperature profiles obtained in the underexpanded round jet with the fluorescence image data is presented.

INTRODUCTION

Laser diagnostics based on molecular scattering provide the experimentalist with non-invasive techniques for probing complex, high-speed flowfields with excellent spatial and temporal resolution. For example, the pulsed lasers used in many experiments have a pulsewidth around 10 nsec so that even in flows of 1 km/sec, fluid molecules move only 10 microns over the pulse duration. With current interest in supersonic combustion attributable to the "national aerospace plane"[1,2] there is an immediate need for the development of laser diagnostics suitable for these high speed, high temperature environments. Of the techniques investigated thus far, laser-induced fluorescence (LIF) is particularly attractive and has been used to measure scalar and vector properties of non-reacting and reacting flows. Previous work has been successful in measuring temperature, pressure, number density and velocity in a variety of compressible flowfields. Temperature measurements have been made in supersonic flows below 300K using LIF of NO seeded into a nitrogen flow[3] and iodine seeded into an air flow.[4] Velocity and pressure fields in supersonic nozzle flows have been determined using the Doppler shift of molecular absorption lines for iodine seeded into a nitrogen flow.[5] All of these results, however, have relied on the introduction of a trace species into the gas flow to facilitate the measurement. In the case of high speed, high temperature flows there is concern over whether such tracers accurately follow the flow[6] and whether the species is chemically stable (will dissociate)[7] or will interfere with the normal reaction chemistry.[8]

An attractive candidate for LIF measurements is molecular oxygen, due to its natural presence (at high levels) in many flows of interest. Although oxygen will be consumed during combustion reactions, and hence its mole fraction may vary in some flows, it is still more desirable than artificial seed species (e.g., Na, I_2, NO) for the reasons mentioned above. Oxygen has not generally been considered as a fluorescent species until recently due to the lack of ultraviolet (uv) laser sources that could excite the strong molecular transitions of the Schumann-Runge band system ($B^3\Sigma_u \leftarrow X^3\Sigma_g$) . With the availability of broadband ArF excimer lasers operating at 193 nm, oxygen imaging becomes practical, having recently been demonstrated in a premixed flame[9] and heated air jet.[10] Currently, excimer lasers can provide tunable, narrowband ($\Delta\upsilon_{FWHM}$ = .004 nm for ArF) uv radiation over a modest range (1 nm) by injection seeding of a stable excimer oscillator into an unstable resonator amplifier; operation in other wavelength regions can be achieved with Raman shifting of the excimer output. The use of a narrowband source has the advantage of providing better overlap with an individual absorption line than broadband ($\Delta\upsilon_{FWHM}$ = .5 nm) excitation, leading to increased signal.

The availability of narrowband uv laser sources also has implications regarding LIF Doppler-shift velocity measurements. Briefly, if there is a component of the gas velocity in the direction of the exciting radiation, the gas molecules absorb at a frequency that is Doppler-shifted from the laser frequency by,

$$\Delta\upsilon_{Doppler} = u / \lambda$$

This shift in frequency changes the absorption coefficient (through the lineshape function), resulting in a proportional change in fluorescent emission intensity. Thus, for suitably narrow laser sources and sufficiently large Doppler shifts, it is possible to infer velocity from LIF signals.[11]

Prominent absorption bands for room temperature oxygen occur in the uv, with continuum absorption occurring below about 175 nm (the vuv) and discrete absorption spectra at longer wavelengths. In this discrete-spectra region each

vibrational band has strong rotational transitions from odd rotational levels, each of which is triplet split, and also weak satellite branches. Recent calculations[12] of absorption coefficients and fluorescence over a range of 300-2000K were used to select an appropriate transition for the experiments reported here. One problem encountered in using 193 nm excitation is in trying to avoid significant laser absorption in the air path between the laser and experiment. To avoid using a purged pathlength, a line was chosen that has negligible absorption at room temperature but displays strongly temperature dependent absorption from 500-1000K. Figure 1 shows the 193 nm oxygen absorption lines at 500K with this line indicated.

The fluorescence signal, S_f, assuming linear (unsaturated) excitation with a narrowband laser is given by,

$$S_f = C\, I\, \chi_{O_2}\, N\, f_b\, [\, A_{21}/(A_{21} + Q)]\, g(\upsilon) \ . \qquad (1)$$

Here C is a constant determined by molecular parameters and the optical arrangement of the experiment, χ_{O2} is the mole fraction of oxygen, N is the total molecular number density, f_b is the temperature-dependent Boltzmann fraction of the absorbing state, $A_{21}/(A_{21} + Q)$ is the ratio of radiative decay to the total decay rate from the upper excited laser level (the Stern-Volmer factor), and $g(\upsilon)$ is the absorption lineshape function which depends on line broadening parameters and the frequency detuning from line center. The quench rate, Q, for oxygen is often dominated by predissociation.[12] Therefore, the Stern-Volmer factor is temperature and pressure independent over a wide range of conditions, and depends only on the upper state vibrational quantum number. Since, for a given upper state, Q can be treated as a constant, the fluorescence signal can be written as,

$$S_f = C'\, N(P,T)\, f_b(T)\, g(\upsilon)\,, \qquad (2)$$

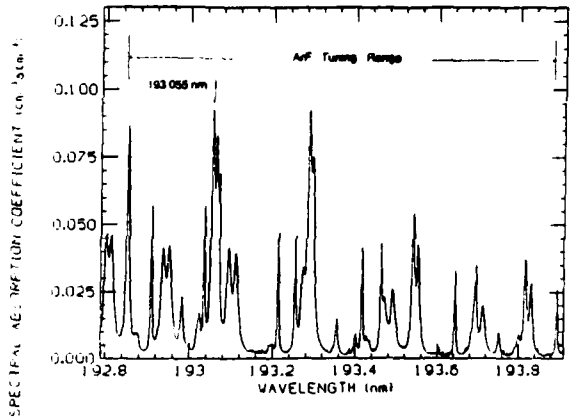

Fig. 1 Oxygen absorption lines at 500K.

where C' is a new constant which includes C, the Stern-Volmer factor, the laser intensity, and the mole fraction of oxygen (taken here to be a constant). In the homogeneously broadened limit (true when the homogeneous linewidth, dominated by predissociation, is much greater than the inhomogeneous linewidth), the lineshape function for line center excitation becomes[13],

$$g(\upsilon_0) = c / Q \ , \qquad (3)$$

where c is a constant. (The effect of non-negligible laser bandwidth can be accounted for within the constant.) Therefore, Eq. (2) can be written for this special case as,

$$S_f \propto N(P,T)\, f_b(T) \ . \qquad (4a)$$

Since N = P / kT, Eq. (4a) becomes,

$$S_f \propto P\, (f_b(T) / T) \propto P\, \alpha(T) \ , \qquad (4b)$$

where α is the absorption coefficient per unit pathlength per unit pressure ($cm^{-1}\ atm^{-1}$). Although it is clear from Eq. (4) that removal of the quenching greatly simplifies the pressure and temperature dependence of the fluorescence signal, the penalty for this is reduction in the signal, a factor that has partially discouraged experimentalists from working with oxygen.

The form of Eq. (4b) suggests that one approach to determine temperature is to select an absorption line that displays a large variation with temperature over the range of temperatures to be measured. For pressure measurements, the converse should be true for the line chosen, that is, the line should be temperature insensitive. For number density measurements, a line would be chosen that displays a small variation in the Boltzmann population fraction with temperature (c.f. Eq. 4a). In order to determine velocity fields, the Doppler shift of the absorption line could be employed as in previous experiments with iodine seeded flows.[5] Proper consideration must be given to the increased linewidths of both the pulsed laser source (relative to past work with cw lasers) and the absorption transitions.

In the present experiments, supersonic imaging of oxygen was performed in an underexpanded round jet of heated air. In this flowfield, pressure and temperature are changing by factors of up to 2 over millimeter distances. By illuminating the flow at 90° to the streamwise axis, Doppler shifts are minimized and thus the fluorescence signal depended on temperature and pressure only.

EXPERIMENTAL PROCEDURE

Experiments were carried out using the heated air issuing from a Sylvania Model SGH 114683 air torch. The torch consists of a quartz tube with an internal heating element over which compressed air is blown. At the end of the tube is a

nozzle with a 1.65 mm orifice. The voltage across the torch was controlled in order to regulate the filament temperature and hence the stagnation temperature of the gas in the heater. The pressurized hot air exited into room air. The upstream-to-background pressure ratio exceeded 1.89, thus the flow at the nozzle exit was underexpanded resulting in a series of rarefaction and shock waves. The flow conditions for the experiments are summarized in Table 1.

The experimental arrangement used here was similar to that used in previous fluorescence experiments. [10] A Lambda-Physik Model 160T MSC excimer laser operating with ArF and tuned to the oxygen absorption transition at 193.055 nm [(7,1)P19] was used as the excitation source. As shown in Figure 2, this transition has negligible room temperature absorption (I/I_0=1/e in 5.9 m of room air) but displays an order of magnitude increase in absorption between 300 and 1000K. A 1 mm air-gap etalon ($\Delta\upsilon_{FSR}$=5 cm^{-1}) with a finesse of 7.3 was used to monitor the bandwidth of the injection-seeded excimer. While operating as a narrowband laser, the output energy was nominally 100 mJ in a 13 nsec pulse. For the experiments reported here, the laser repetition rate was 11 Hz. Pulse-to-pulse energy fluctuations were measured to be within ± 6 %. A 38 cm focal length cylindrical lens and 100 cm spherical lens, both made of uv-grade fused silica, were used to create a sheet of light in a horizontal plane approximately 100 μm thick. The sheet was steered to just touch the exit plane of the glass nozzle at the midplane of the flow. A graphite block was used as the beam stop. The fluorescence was imaged at 90° to the laser sheet. A 3 mm thick piece of KBr was used as a long-pass filter to block elastically scattered light from entering the collection optics.

Table 1 Summary of flow conditions

PROPERTY \ REGION	Run no.	Stagnation (0)	Nozzle Exit (*)	Background Pocket (b)	Maximum Mach Number (m)
Pressure (Torr)	1	1640	866	760	694
	2	1900	1004	760	623
	3	2136	1128	760	587
Temperature (K)	1	1060	675	842	821
	2	1060	675	809	763
	3	1060	675	782	715
Mach Number	1	0	1	1.11	1.18
	2	0	1	1.22	1.37
	3	0	1	1.31	1.53

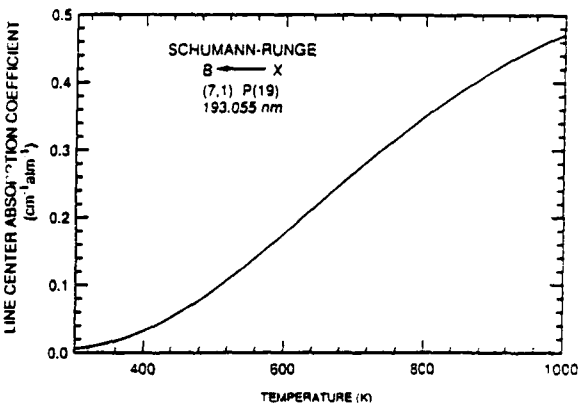

Fig. 2 Line-center absorption coefficient.

In order to maximize fluorescence light collection, it is desirable to mount the imaging lenses as close to the experiment as possible, thus increasing the collection solid angle. Hence, two uv 105 mm focal length Nikkor lenses (*f*/4.5), mounted back-to-back and focused at infinity, were used to perform 1:1 imaging. The lenses were mounted to an adapter ring holding an ITT Model 4144 dual-plate image intensifier with an S-20 photocathode. The image intensifier is used to obtain shot-noise limited operation at the low light levels typical of oxygen fluorescence experiments. The intensifier was mounted to a Reticon Model MC520 100x100 element array camera using fiberoptic bundle coupling. The 1:1 imaging resulted in fluorescence from a 6mm square region of the flowfield being imaged onto the array.

The Reticon camera data was acquired using a Microtex 7402 camera/computer interface hosted in an LSI-11 laboratory computer. Display of the camera output was via a Lexidata color graphics monitor. Data manipulation including background subtraction, frame and/or pixel averaging, and rescaling was performed in software.

RESULTS AND DISCUSSION

For each experimental condition given in Table 1, 24 frames of data were acquired at 11 Hz using an intensifier gate width of 2 μsec. From the 24 images, a sequence of 8 was chosen as best representing the flow. Twenty-four background frames were also acquired; these frames are used to account for integrated dark current, odd/even row imbalances in the array, and background scattered light. The average of these background frames was subtracted from each of the eight flow frames and then these background-corrected frames were averaged. A 3x3 pixel spatial average was then performed to improve image quality. The resulting images, displayed in 5 grey levels, are shown in Figure 3.

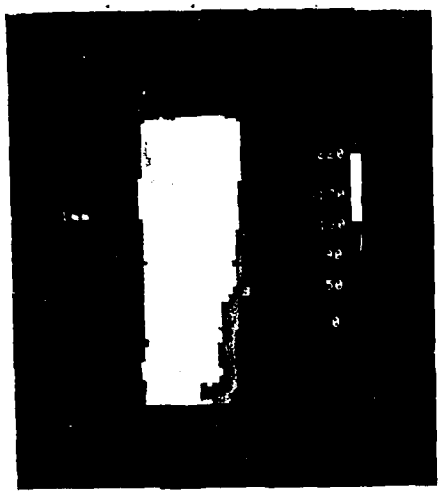

(a)

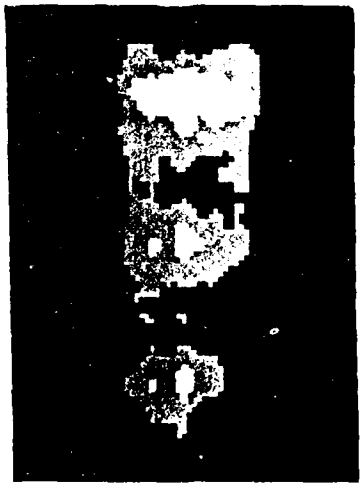

(b)

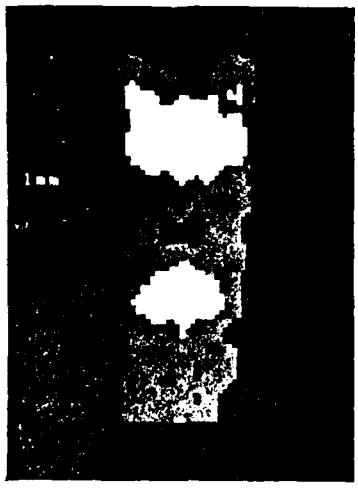

(c)

Fig. 3 Fluorescence images for P_0 / P_b = (a) 2.2, (b) 2.5, and (c) 2.8. The grey scale (arbitrary units) is shown in (a).

The flowfield of an underexpanded round jet is well understood.[14] For upstream-to-background pressure ratios exceeding about 1.9, a supersonic regime with a periodic diamond pattern of shock waves and expansion fans is encountered (Figure 4). Above a pressure ratio of about 5, a strong normal shock ('Mach disk') appears and the jet behavior becomes strongly non-isentropic. At the highest pressure ratio used here, 2.8, the flow was still nearly isentropic with no Mach disk appearing. The method of characteristics can be used to determine the expected temperature and pressure values in the first few regions of the two-dimensional diamond pattern. In the simplest analysis, the expansion fans are approximated as a single Mach wave and isentropic flow calculations are used to establish the peak conditions in each "cell". Beyond the jet near-field (i.e., the first few shock cells), the inviscid calculations are no longer accurate and turbulent mixing with the surrounding fluid must be accounted for.[15]

The images of oxygen fluorescence in a supersonic flow are related to the change in pressure and temperature as the underexpanded jet accommodates to its surroundings. Qualitatively, the images in Figure 3 show the repetitive diamond pattern expected for this flowfield. As the pressure ratio is increased, the spacing between the cells also increased, consistent with theory. The pattern of alternating high-to-low pressure and temperature (low-to-high velocity) would repeat exactly except for mixing with the surrounding gas which serves to decrease the amplitude of the fluctuations. However, for the first few cells, it is reasonable to assume that the changes in pressure, temperature, and velocity are small[15] and that the calculated values for these variables correspond to the peak measured values in the experiments.

Figure 5 shows a cut along the flow axis for each of the experiments and the variation in fluorescence amplitude along that cut. The peaks and valleys correspond to regions of the flow where pressure and temperature alternate between high and low values in the nozzle exit (*) and maximum mach number (m) regions, respectively. The ratios of the maximum

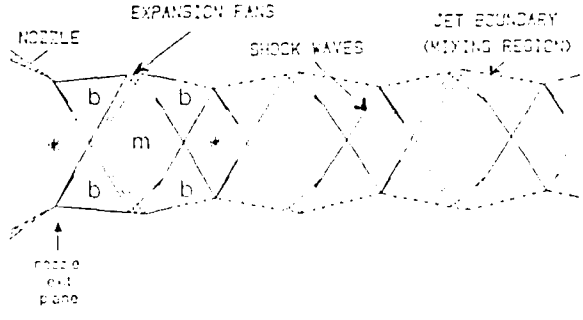

Fig. 4 Geometry of an underexpanded, supersonic jet.

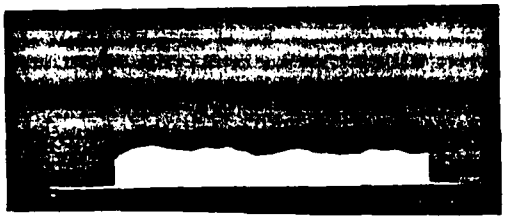

(a)

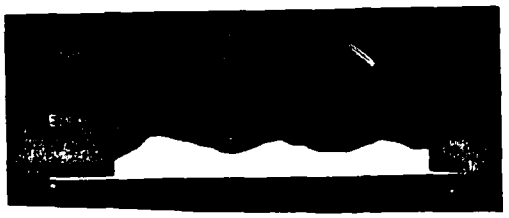

(b)

(c)

Fig. 5 Fluorescence variation along the flow axis for the three test conditions.

to minimum fluorescence signals at each test condition in Figure 5 compare favorably with theoretical predictions of fluorescence ratios for the known pressure and temperature in each cell. For the three flow conditions tested, these ratios were measured as 1.5, 2.0, and 2.5. Using the calculated temperatures from Table 1 to determine the absorption coefficient (cm^{-1} atm^{-1}) from Figure 2, and then multiplying by the pressures (also from Table 1), the corresonding fluorescence ratios were calculated as 1.4, 2.1, and 3.0.

CONCLUSIONS

Oxygen fluorescence images have been acquired in supersonic flows, demonstrating temperature and pressure sensitivity. The technique can be modified to enable imaging a single flowfield property. For example, to measure pressure fields, an absorption line that is insensitive to temperature can be used. In isentropic flows (flows with weak shocks), the temperature and pressure are related through isentropic relationships so that after imaging the pressure field, the temperature field can be calculated. All of the above applies to non-reacting flows where the mole fraction of oxygen is constant. If this is not true, as in reacting flows, the measurement can be used to determine oxygen number density. Multiple measurements (e.g. with two excitation wavelengths and broadband collection, or a single excitation wavelength with two detection channels) can also be used to allow combined measurements of multiple parameters in reacting flows.

Additional facilities are being considered for future experiments, such as a supersonic shear layer and a hypersonic shock tunnel. For velocity imaging in oxygen using Doppler-shifted absorption, there are a number of additional considerations. At 193 nm there is a Doppler shift of 5 GHz per 1 km/sec of velocity, or a shift of .0006 nm from the excitation wavelength. At 1000K, for example, the triplets in each of the 193 nm absorption lines are partially overlapping, resulting in an observed feature linewidth of $\Delta\upsilon \geq .005$ nm. The change in absorption, due to the above calculated Doppler shift, would be difficult to observe at these conditions. Absorption lines at 179 nm (corresponding to one anti-stokes Raman shift of ArF in hydrogen), however, are narrower and more spectrally separated so that the Doppler shift could be determined from the change in absorption (fluorescence) on a single line of the triplet. In addition, absorption coefficients for these lines are 10 or more times higher than at 193 nm. Although the laser energy will be reduced in the stimulated Raman process, the fluorescence signal should still be enhanced due to the stronger absorption coefficient.

ACKNOWLEDGEMENT

This research was supported by the U. S. Air Force Office of Scientific Research under contract F49620-83-K-0004.

REFERENCES

[1]Williams, R. M., "National Aero-Space Plane: Technology for America's Future," *Aerospace America*, Nov. 1986, pp. 18-22.

[2]Korthals-Altes, S. W., "Will the Aerospace Plane Work? " *Technology Review*, Jan. 1987, pp. 43-51.

[3]Gross, K. P. and McKenzie, R. L., "Measurements of Fluctuating Temperatures in a Supersonic Turbulent Flow Using Laser-Induced Fluorescence," *AIAA Journal*, Vol. 23, Dec. 1985, pp. 1932-1936.

[4]Fletcher, D. G. and McDaniel, J. C., "Temperature Measurement in a Compressible Flow Using Laser-Induced Iodine Fluorescence," *Optics Letters*, Vol. 12, Jan. 1987, pp. 16-18.

[5]Hiller, B., Cohen, L. M., and Hanson, R. K., "Simultaneous Measurements of Velocity and Pressure Fields in Subsonic and Supersonic Flows Through Image-Intensified Detection of Laser-Induced Fluorescence," *AIAA Paper* 86-0161, 1986.

[6]Teshima, K., "Visualization for a Free Jet by a Laser-Induced Fluorescence Method and its Structure," *Proceedings of the Symposium on Mechanics for Space Flight*, Tokyo, Japan, 1983.

[7]Beck, N. J., Chen, S. K., Uyehara, O. A., Winans, J. G., and Myers, P. S., "Temperature Measurements from Iodine Absorption Spectrum," *Fifth Symposium (International) on Combustion*, The Combustion Institute, Pittsburgh, PA, 1954, pp. 412-423.

[8]Hynes, A. J., Steinberg, M., and Schofield, K., "The Chemical Kinetics and Thermodynamics of Sodium in Oxygen-Rich Hydrogen Flames," *Journal of Chemical Physics*, Vol. 80, 15 March 1984, pp. 2585-2597.

[9]Lee, M. P., Paul, P. H., and Hanson, R. K., "Laser-Fluorescence Imaging of O_2 in Combustion Flows Using an ArF Laser," *Optics Letters*, Vol. 11, Jan. 1986, pp. 7-9.

[10]Lee, M. P., Paul, P. H., and Hanson, R. K., "Quantitative Imaging of Temperature Fields in Air Using Planar Laser-Induced Fluorescence of O_2," *Optics Letters*, Vol. 12, Feb. 1987, pp. 75-77.

[11]Hiller, B. and Hanson, R. K., "Two-Frequency Laser-Induced Fluorescence Technique for Rapid Velocity-Field Measurements in Gas Flows," *Optics Letters*, Vol. 10, May 1985, pp. 206-208.

[12]Lee, M. P. and Hanson, R. K., "Calculations of O_2 Absorption and Fluorescence at Elevated Temperatures for a Broadband Argon-Fluoride Laser Source at 193 nm," *Journal of Quantitative Spectroscopy and Radiative Transfer*, Vol. 36, 1986, pp. 425-440.

[13]Piepmeier, E. H., "Theory of Laser Saturated Atomic Resonance Fluorescence," *Spectrochemica Acta*, Vol. 27B, 1972, pp. 431-443.

[14]Thompson, P. A., Compressible-Fluid Dynamics, McGraw-Hill, 1972, pp. 462-464.

[15]Dash, S. M., Wolf, D. E., and Seiner, J. M., "Analysis of Turbulent Underexpanded Jets, Part I: Parabolized Navier-Stokes Model, SCIPVIS," *AIAA Journal*, Vol. 23, April 1985, pp. 505-514.

END

12-87

DTIC